Journal of Alloys and Compounds 509 (2011) 1448–1451

Contents lists available at ScienceDirect

Journal of Alloys and Compounds

journal homepage: www.elsevier.com/locate/jallcom

Competition between interfacial and interlayer exchange couplings in $Co/Cr_2O_3/Fe$ trilayers

X.H. Liu, W. Liu*, S. Guo, X.K. Lv, W.J. Gong, Z.D. Zhang

Shenyang National Laboratory for Materials Science and International Centre for Materials Physics, Institute of Metal Research, Chinese Academy of Sciences, 72 Wenhua Road, Shenyang 110016, Liaoning, PR China

ARTICLE INFO

Article history:
Received 7 September 2010
Received in revised form
12 November 2010
Accepted 17 November 2010
Available online 23 November 2010

Keywords:
Interfacial and interlayer exchange couplings
$Co/Cr_2O_3/Fe$ trilayers
Magnetotransport properties

ABSTRACT

The temperature dependence of competition between interlayer and interfacial couplings is observed at different temperatures in Co (3 nm)/Cr_2O_3 (t)/Fe (10 nm) trilayers with t = 3 nm, 6 nm, 15 nm and 25 nm, respectively. The interlayer coupling enhances and the interfacial coupling weakens with increasing temperature. The balanceable temperature between interfacial and interlayer couplings shifts to low temperatures with increasing spacer thickness. Furthermore, the competition between interfacial and interlayer couplings greatly affects the magnetotransport properties of the trilayers. The negative magnetoresistance and the minimum resistance corresponding to balanceable temperature are found in trilayers.

1. Introduction

The study on the interlayer exchange coupling between ferromagnetic (FM) films separated by a nonmagnetic (NM) metal layer has been the key factor for the discovery of giant magnetoresistance [1–5]. In metallic systems, exchange interactions are propagated by itinerant electrons, which can be transmitted over long distances, as well understood with a Ruderman–Kittel–Kasuya–Yosida-type (RKKY) coupling modified by the discreteness of spacer materials [6]. For insulating spacer, non-oscillatory decay of the interlayer coupling strength with spacer thickness has been observed [7], which can be interpreted by the models [8,9]. In contrast, the oscillatory of the interlayer exchange coupling is found in $[Pt/Co]_3/NiO/[Pt/Co]_3$ multilayers [10], in which the antiferromagnetic (AF) ordering of insulator spacer layer plays very important role. In previous work, a noncollinear alignment was found in magnetization directions of the two FM layers, and a spiral spin structure of AF results in different angles between the magnetization axes of two FM layers in FM/AF/FM trilayers [11–14]. In these systems, top and bottom FM layers are identical, which leads to the difficulty for separating magnetization contributions of two FM layers in the M–H curves [13]. On the other hand, different magnetic anisotropies of FM layers could be used, in order to observe a spiral spin structure within AF layer, and the 90° coupling between two FM layers [12,14]. From studying the micromagnetic structure of magnetic domains in trilayers, small magnetic domains were observed to be separated by nanometer-sized domain walls in the top of Fe for a narrow CoO thickness range [15]. The Co–Fe interlayer exchange coupling changes from a 90° coupling ($d_{NiO} < 2$ nm) to a collinear one ($d_{NiO} > 2$ nm) with increasing the NiO thickness in Co/NiO/Fe sandwich [16]. Furthermore, the competition between interlayer and interfacial couplings is observed in FM/AF/FM trilayers with AF metallic and insulating spacer materials [17,18]. However, the effect of spacer thickness in FM/AF/FM trilayers is needed to study further.

In this paper, we report the observation of the competition between interfacial coupling in FM/AF and interlayer coupling in $Co/Cr_2O_3/Fe$ trilayers with different spacer thicknesses at different temperatures. Furthermore, the magnetotransport properties of trilayers are greatly affected by the competition between interfacial coupling between FM and AF layers and interlayer coupling between two FM layers.

2. Experimental

The growth of the films was carried out in a high-vacuum chamber equipped with multi-sputtering guns. The base pressure of the chamber was better than 2×10^{-7} Torr. Ar gas was kept at a pressure of 4×10^{-3} Torr during sputtering. A target with commercial Pt, Co, Cr_2O_3 and Fe targets with 99.99% purity was used. The trilayers Co (3 nm)/Cr_2O_3 (t)/Fe (10 nm) with spacer thickness t = 3 nm, 6 nm, 15 nm, and 25 nm were prepared by DC and RF magnetron sputtering. First, a 10 nm Pt buffer layer was grown onto a Si substrate, then the Co (3 nm)/Cr_2O_3 (t)/Fe (10 nm) trilayers was deposited onto it, and finally, one additional 5 nm Pt layer was deposited on the top for the prevention of oxidation. The crystal structure was investigated by means

* Corresponding author. Tel.: +86 24 83978856; fax: +86 24 23891320.
E-mail address: wliu@imr.ac.cn (W. Liu).

0925-8388/$ – see front matter © 2010 Published by Elsevier B.V.
doi:10.1016/j.jallcom.2010.11.111

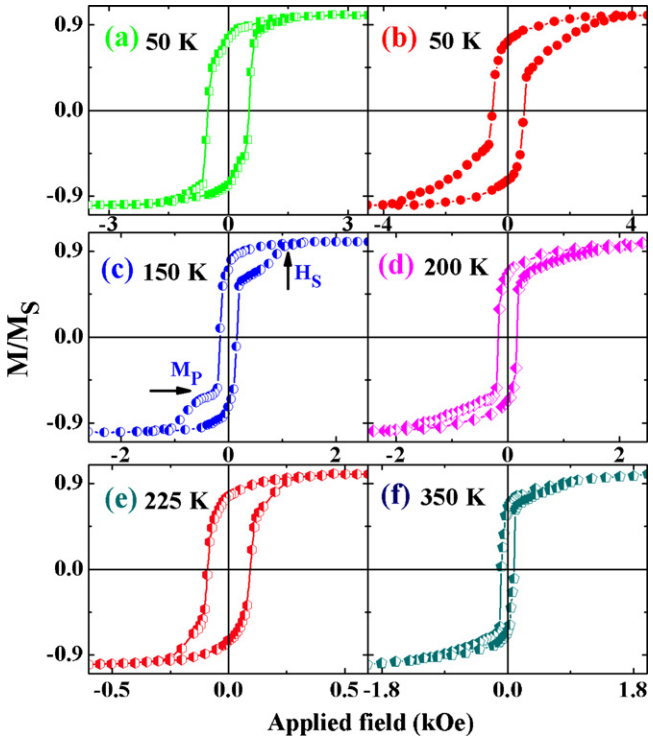

Fig. 1. Magnetic hysteresis loops at 50 K (a), 150 K (c), 225 K (e), of Co (3 nm)/Cr_2O_3 (3 nm)/Fe(10 nm), and at 50 K (b), 200 K (d), 350 K (f), of Co (3 nm)/Cr_2O_3 (25 nm)/Fe (10 nm) after ZFC.

of X-ray diffraction (XRD) with Cu K_α radiation. The magnetic properties at different temperatures were measured using a superconducting quantum interference device (SQUID). The hysteresis loops were recorded after zero-field-cooling (ZFC) and field-cooling (FC) processes, cooling from room temperature to 10 K and from 350 K to 10 K, respectively. A series of the hysteresis loops were obtained during warming up, which were normalized by saturation magnetization (M_S). The resistance and magnetotransport properties were measured using standard four-probe dc method, while warming.

3. Results and discussion

In order to investigate the temperature dependence of magnetic properties, the magnetic hysteresis loops measured at 50 K, 150 K, 225 K for t = 3 nm and 50 K, 200 K, 350 K for t = 25 nm after ZFC are presented in Fig. 1(a), (c), (e) and (b), (d), (f), respectively. It is found from Fig. 1(a) that the hysteresis loop exhibits well coupling between FM layers across the AF spacer at 50 K. At 150 K, a step of magnetization (M_P) appears and then it jumps to the saturation magnetization M_S at the saturation field (H_S), where, M_P and H_S are indicated by arrows in Fig. 1(c). Moreover, the disappearance of step at $T \geq 225$ K indicates the FM coupling between two FM layers. However, it is found that the magnetization increases with increasing H in the first quadrant (symmetry in the third quadrant) with M_P = 0.36 at 50 K for t = 25 nm in Fig. 1(b), while no clear FM coupling observed even at $T \geq 350$ K is suggestive of quite weak interlayer coupling for this sample. The magnetic moment per Fe atom is 2.22μ_B and that per Co is 1.72μ_B [19]. For the antiparallel alignment of the moments of two FM layers, the M_P is about 0.6. For sample with t = 25 nm, the values of M_P = 0.36 at 50 K and $M_P \approx 0.6$ at $T \geq 200$ K mean the partial reversal of Fe layer and antiparallel of Fe and Co layers at step, respectively.

The hysteresis loops at 10 K of trilayers with different spacer thicknesses 3 nm, 6 nm, 15 nm and 25 nm after ZFC (solid symbol) and FC (open symbol) are presented in Fig. 2(a)–(d), respectively. It is found that two FM layers are well coupled after ZFC for the trilayers with spacer thickness of 3 nm and 6 nm. But the steps are clear

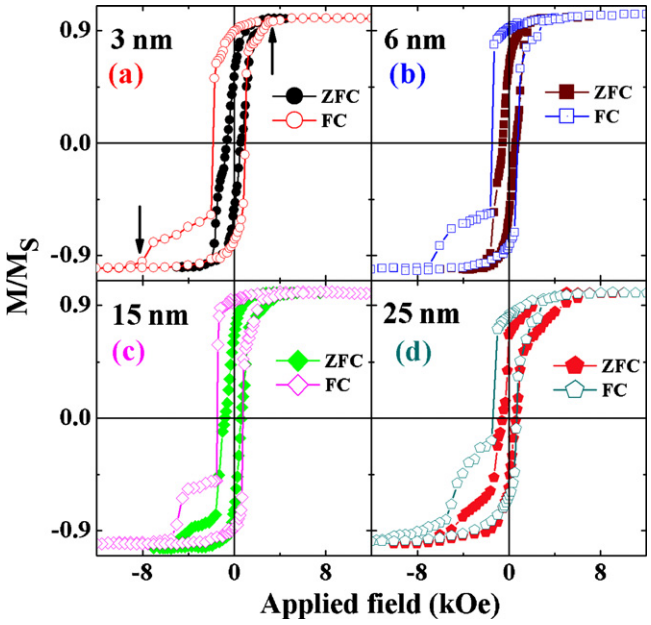

Fig. 2. Magnetic hysteresis loops at 10 K for t = 3 nm (a), 6 nm (b), 15 nm (c) and 25 nm (d) after ZFC and FC, of Co (3 nm)/Cr_2O_3 (t)/Fe (10 nm).

for t = 15 and 25 nm, indicating weak interfacial coupling between AF and FM layer for thicker spacer. For FC case, all the trilayers exhibit steps in the third quadrant with different values of H_S and no step in the first quadrant. H_S in the third quadrant is defined as H_{S3}, and in the first quadrant H_{S1} (as arrows indicate). The asymmetrical coefficient $L = H_{S3}/H_{S1}$ is defined. L = 1 means symmetrical loops, suggesting that the interfacial coupling between FM and AF layers is quite weak after FC [20]. The curves of L versus T with spacer thickness of 3, 6, 15 nm are presented in Fig. 3. It is noticed that the values of L decrease with increasing spacer layer at low T, indicating stronger interfacial coupling for thinner spacer, moreover, $L \approx 1$ for t = 15 nm at the lower temperature also confirms the weaker interfacial coupling for thicker spacer layer.

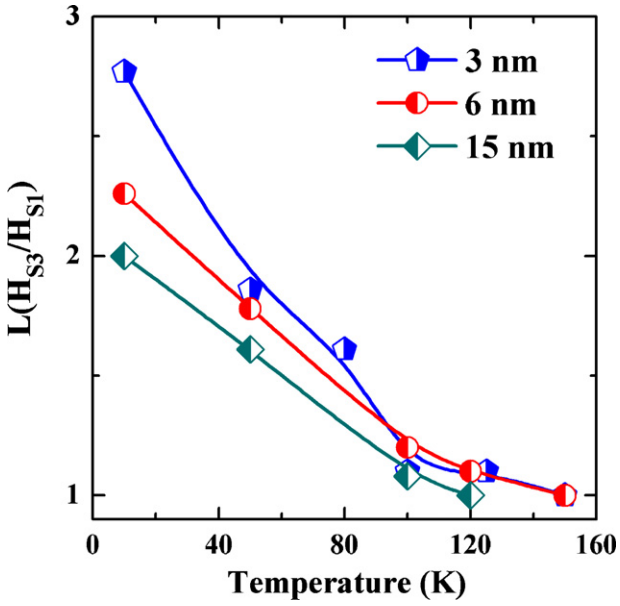

Fig. 3. The temperature dependence of asymmetrical coefficient L for samples with t = 3 nm, 6 nm and 15 nm.

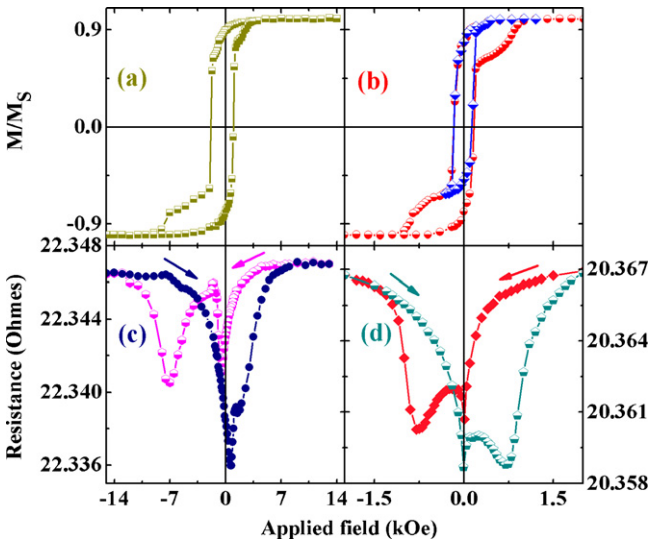

Fig. 4. Magnetic loop at 10 K (a), the major and minor loops at 150 K (b), the *R*–*H* curve at 10 K (c), and *R*–*H* curve at 150 K (d), of Co (3 nm)/Cr_2O_3 (3 nm)/Fe (10 nm) after FC.

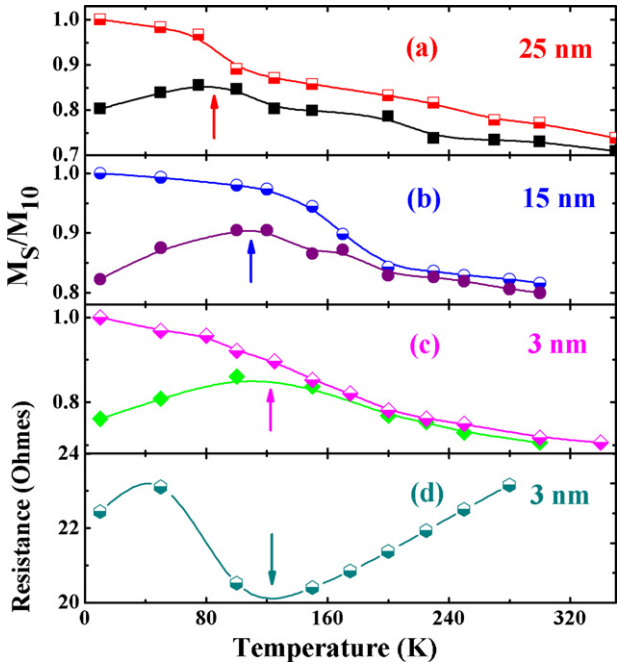

Fig. 5. Temperature dependence of saturation magnetization for t = 25 nm, 15 nm and 3 nm after ZFC and FC, and saturation R for 3 nm after ZFC, respectively, of Co (3 nm)/Cr_2O_3 (t)/Fe (10 nm). The arrow indicates the peak temperature of ZFC curve and saturation R.

To further clarify the relationship between magnetization orientation of FM layers and spin-dependent scattering magnetoresistance (*MR*), the resistance (*R*) and magnetic hysteresis loops for 3 nm after FC are shown in Fig. 4. This figure exhibits hysteresis loop at 10 K (Fig. 4(a)), major/minor loops at 150 K (Fig. 4(b)), *R*–*H* curve at 10 K (Fig. 4(c)), and *R*–*H* curve at 150 K (Fig. 4(d)). The negative *MR* is observed at the coercivity field in Fig. 4(c), and the sharp decrease/increase of *R* corresponds to the first/second sharp switching in the hysteresis loop, respectively. The plateau of *R* corresponds to the step of the field-decreasing branch in the third quadrant, and the second minimum of *R* corresponds to the magnetization reversal of the Co layer at about −8 kOe in Fig. 4(a). However, it is clear from Fig. 4(b) and (d) that the two plateaus of *R* corresponding to the two steps in hysteresis loop are different from those at 10 K, suggesting the strong influence of interfacial exchange coupling on the spin-dependence scattering. The interlayer coupling (sign and strength) between the Co and Fe layers can be determined by minor-loop measurements (as shown in Fig. 4(b)). The minor-loop shift $H_E < 0$ means the FM coupling, while $H_E > 0$ is indicative of the AF coupling, and the interlayer coupling strength of the trilayers can be expressed as $J_E = H_E M_S t_{FM}$ [10], where M_S and t_{FM} are the saturation magnetization and the thickness of the Fe layer, respectively. All the values of $H_E < 0$ mean the FM coupling between FM layers for all the trilayers, and small values of H_E mean weak interlayer coupling strength in trilayers in the temperature range.

The temperature dependence of M_S after ZFC and FC for t = 25 nm, 15 nm and 3 nm and saturation R after ZFC (nearly the same values of saturation R for ZFC and FC cases) for t = 3 nm are presented in Fig. 5. As the M_S is the largest after FC at 10 K for each sample, each curve of Fig. 5 is normalized by M_S after FC at 10 K. It is found that the value of M_S for every sample after ZFC exhibits a peak at different temperatures (as arrows indicated), but it decreases with increasing temperature for every one after FC. Meanwhile, the peak temperature (T_P) of ZFC curve shifts to low temperature with increasing spacer thickness. In Fig. 5(c) and (d), the maximum of M_S after ZFC corresponds to the minimum of saturation R at T_P, indicating that the competition between interfacial coupling between FM and AF layers and interlayer coupling between two FM layers greatly influence the magnetotransport properties of trilayers.

We study the total free energy E to discuss the mechanism of exchange coupling in the Co/Cr_2O_3/Fe trilayers. There are four contributions to the total free energy of trilayers, whereas, the main contributions to the variation of the free energy with temperature come from the interlayer coupling in trilayers and the interfacial coupling between FM and AF layers in the temperature range we are interested in Ref. [17]. The competition of these two couplings leads to a rather strong temperature dependence of the coupling. Recently, several studies were carried out on the temperature dependence of magnetic coupling via metallic or insulating layers [10,21,22]. $J(T) = J(0\,K)(T/T_0)/(\sinh(T/T_0))$. Here, $J(0\,K)$ is the interlayer coupling strength at T = 0 K, $T_0 = \hbar\upsilon_F/2\pi k_B d$ is the characteristic temperature, d being the thickness of the spacer [21], in which the interlayer coupling strength monotonously decreases/increases for metal/insulator spacer with increasing temperature [8]. The exchange bias field H_{EX} decreases with increasing temperature [23], and the interfacial coupling energy $J_{EX} = H_{EX} M_S t_{FM}$, M_S and t_{FM} are the saturation magnetization and the thickness of the FM layer, respectively [24]. It is found that the interlayer coupling strength increases and the interfacial coupling strength decreases for AF insulator spacer Cr_2O_3. Moreover, the J_{EX} of the Co/Cr_2O_3/Fe trilayers would be approximately considered to decrease with increasing temperature [25].

For ZFC case, the interfacial coupling in AF/FM would play the dominant role at low temperatures. The interfacial coupling between Co/Cr_2O_3 and Fe/Cr_2O_3 will not be FM or AF after ZFC, and the two branches are nearly symmetric (shown in Fig. 1). When the interfacial coupling is strong enough, the reversal of Fe and Co layers will simultaneously occur (see Fig. 2(a) and (b) for t = 3 nm and 6 nm, respectively). However, for trilayers with thicker spacer (see Fig. 2(c) and (d)), the interfacial coupling between FM/AF is not strong enough to switch all the Co layer with reversal of Fe layer, because the strength of the interfacial coupling in AF/FM decreases with increasing AF thickness [26], and step-like hysteresis loops after ZFC are found. With an increase of temperature, only partial Co layer switches with the reversal of Fe in applied field due to the reduction of the interfacial exchange coupling, leading to the

appearance of a step in the hysteresis loop for $t = 3$ nm (Fig. 1(c)) and 6 nm. When $T > T_P$, the FM interlayer coupling will gradually dominate the couplings, accordingly, the step gradually disappears with increasing temperature [27]. For the FC case, the moments of FM layers and the interface of AF layers tend to the direction of external field, and the strong FM coupling in FM/AF occurs at low temperatures (see the negative exchange bias field in Fig. 2). For the increasing-field branch, the moments of FM layers reverse at smaller field in order to reduce the interfacial energy (FM coupling of FM/AF interface is in a low energy state). The stronger exchange coupling in Co/Cr_2O_3 is, the more instable in Co/Cr_2O_3 interface [20], which would lead to moments' reversal of Co and Fe layers at the same field in Fig. 2 [28]. A clear step appears in the first quadrant with increasing temperature due to decrease of interfacial coupling between Co and Cr_2O_3 layers. In addition, weak interlayer coupling for $t = 25$ nm leads to disappearance of FM coupling in the magnetic hysteresis loop even at 350 K.

It is found from Fig. 1 that the magnetization varies from step to M_S with a linear-like increase rather than a sharp jump, which exhibits spin-flop-like behavior. There are three parts in our system: the Fe layer as FM_1, the spacer Cr_2O_3, and the FM_2 Co. Therefore, for this system, when a step appears, we can assume the two sublattices (corresponding to the spins moments of two FM layers) with antiparallel spins as an AF material, in which both the sublattices have easy anisotropy at in-plane. The field applied parallel to the direction of the sublattice magnetization may lead to an instability of the ground state of AF material, if the strength H exceeds the value $H_{cr} = (2H_{EC}H_A)^{1/2}$, at $T = 0$. Here H_{EC} and H_A are interlayer exchange coupling and intralayer uniaxial anisotropy, respectively [29]. Therefore, the moments' directions of Fe and Co gradually vary when external field is larger than H_{cr}, and the spin-flop-like phenomenon will occur. The experimental results at low bias are generally interpreted according to Jullière's expression, $\Delta R/R = (R_{AP} - R_P)/R_{AP} = 2P_1P_2/(1 + P_1P_2)$, where R_{AP} and R_P are the resistances in the antiparallel and parallel states, respectively, and the P_1 and P_2 are the electron spin polarizations of the two electrodes [30]. The negative magnetoresistance presented in Fig. 4 is indicative of the different signs of the electron spin polarizations of Co and Fe electrodes. Moreover, the values of R in Figs. 4(c) and (d) indicate that the interfacial coupling and interlayer coupling greatly affect the magnetotransport properties of trilayers.

Furthermore, the interlayer coupling between two FM layers increases and the interfacial coupling between AF and FM decreases with increasing temperature. Therefore, there would be a balance between these two couplings at a critical temperature (T_{cr}). The interfacial coupling is dominant at $T < T_{cr}$, but the interlayer coupling becomes dominant at $T > T_{cr}$, and the FM interlayer coupling will increase M_P, and the decrease of M_S may be due to the thermal effect [17]. As a result, the T_P for ZFC case in Fig. 5 corresponds to this critical temperature, at which a clear step appears in M–H loop (see Fig. 1). As interfacial and interlayer couplings are weak for thick spacer layer, thus, the lower T_P indicates a new balance between two couplings at low temperatures. Moreover, the minimum of saturation R at T_P in Fig. 5(d) indicates the influence of competition between interfacial and interlayer coupling on saturation R.

4. Conclusion

The temperature dependence of interlayer and interfacial exchange couplings is observed by measuring hysteresis loops at different temperatures in Co (3 nm)/Cr_2O_3 (t)/Fe (10 nm) trilayers with $t = 3$ nm, 6 nm, 15 nm and 25 nm, respectively. The balanceable temperature between interfacial and interlayer couplings shifts to low temperatures with increasing spacer thickness. Furthermore, the competition between interfacial coupling between FM and AF layers and interlayer coupling between two FM layers greatly affects the magnetotransport properties of trilayers.

Acknowledgements

This work has been supported by the National Basic Research Program (No. 2010CB934603) of China, Ministry of Science and Technology of China and the National Nature Science Foundation of China under projects 50931006 and 50971123.

References

[1] P. Grünberg, R. Schreiber, Y. Pang, M.B. Brodsky, H. Sowers, Phys. Rev. Lett. 57 (1986) 2442.
[2] M.N. Baibich, J.M. Broto, A. Fert, F. Nguyen Van Dau, F. Petroff, P. Etienne, G. Creuzet, A. Friederich, J. Chazelas, Phys. Rev. Lett. 61 (1988) 2472.
[3] R.W. Wang, D.L. Mills, Phys. Rev. Lett. 72 (1994) 920.
[4] Y. Wang, P.M. Levy, J.L. Fry, Phys. Rev. Lett. 65 (1990) 2732.
[5] S.S. Parkin, N. More, K.P. Roche, Phys. Rev. Lett. 64 (1990) 2304.
[6] P. Bruno, C. Chappert, Phys. Rev. Lett. 67 (1991) 1602.
[7] J.F. Vincent, C. Tiusan, C. Bellouard, E. Popova, M. Hehn, F. Montaigne, A. Schuhl, Phys. Rev. Lett. 89 (2002) 107206.
[8] P. Bruno, Phys. Rev. B 52 (1995) 411.
[9] J.C. Slonczewski, Phys. Rev. B 39 (1989) 6995.
[10] Z.Y. Liu, S. Adenwalla, Phys. Rev. Lett. 91 (2003) 037207.
[11] J.C. Slonczewski, Phys. Rev. Lett. 67 (1991) 3172.
[12] F.Y. Yang, C.L. Chien, Phys. Rev. Lett. 85 (2000) 2597.
[13] P.A.A. van der Heijden, C.H.W. Swüste, W.J.M. de Jonge, J.M. Gaines, J.T.W.M. van Eemeren, K.M. Schep, Phys. Rev. Lett. 82 (1999) 1020.
[14] J. Camarero, Y. Pennec, J. Vogel, M. Bonfim, S. Pizzini, F. Ernult, F. Fettar, F. Garcia, F. Lancon, L. Billard, B. Dieny, A. Tagliaferri, N.B. Brookes, Phys. Rev. Lett. 91 (2003) 027201.
[15] A. Brambilla, P. Sessi, M. Cantoni, M. Finazzi, N. Rougemaille, R. Belkhou, P. Vavassori, L. Duòand, F. Ciccacci, Phys. Rev. B 79 (2009) 172401.
[16] J. Wu, J. Choi, A. Scholl, A. Doran, E. Arenholz, Y.Z. Wu, C. Won, C.Y. Hwang, Z.Q. Qiu, Phys. Rev. B 80 (2009) 012409.
[17] X.H. Liu, W. Liu, F. Yang, X.K. Lv, W.B. Cui, S. Guo, W.J. Gong, Z.D. Zhang, Appl. Phys. Lett. 95 (2009) 222505.
[18] X.H. Liu, W. Liu, S. Guo, F. Yang, X.K. Lv, W.J. Gong, Z.D. Zhang, Appl. Phys. Lett. 96 (2010) 082501.
[19] E.P. Wohlfarth (Ed.), Handbook of Magnetic Materials, vol. 1, North-Holland, Amsterdam, 1980, Chapter 1.
[20] J. Nogués, J. Sort, V. Langlais, V. Skumryev, S. Suriñach, J.S. Muñoz, M.D. Baró, Phys. Rep. 422 (2005) 65.
[21] J. Lindner, C. Rüdt, E. Kosubek, P. Poulopoulos, K. Baberschke, P. Blomquist, R. Wäppling, D.L. Mills, Phys. Rev. Lett. 88 (2002) 167206.
[22] K.M. Döbrich, M. Wietstruk, J.E. Prieto, F. Heigl, O. Krupin, K. Starke, G. Kaindl, Phys. Rev. Lett. 100 (2008) 227203.
[23] A.P. Malozemoff, Phys. Rev. B 35 (1987) 3679.
[24] W.H. Meiklejohn, J. Appl. Phys. 29 (1958) 454.
[25] J. Sort, B. Dieny, J. Nogués, Phys. Rev. B 72 (2005) 104412.
[26] V. Baltz, J. Sort, S. Landis, B. Rodmacq, B. Dieny, Phys. Rev. Lett. 94 (2005) 117201.
[27] X.H. Liu, W. Liu, S. Guo, W.J. Gong, J.N. Feng, Z.D. Zhang, Appl. Phys. Lett. 97 (2010) 072502.
[28] M.G. Blamire, M. Ali, C.W. Leung, C.H. Marrows, B.J. Hickey, Phys. Rev. Lett. 98 (2007) 217202.
[29] D.L. Mills, Phys. Rev. Lett. 20 (1968) 18.
[30] J.M. De Teresa, A. Barthelemy, A. Fert, J.P. Contour, F. Montaigne, P. Seneor, Science 286 (1999) 507.